Published in Journal of Electroanalytical Chemistry 1999, vol 472, p 42-52
doi:10.1016/S0022-0728(99)00259-4

Voltammetric currents for any ligand-to-metal concentration ratio in fully labile metal-macromolecular complexation. Easy computations, analytical properties of the currents and a graphical method to estimate the stability constant.

Josep GALCERAN[a*], Joan CECILIA[b], José SALVADOR[a] , Josep MONNÉ[a], Marià TORRENT[a], Encarnació COMPANYS[a], Jaume PUY[a]

[a] Departament de Química, [b] Departament de Matemàtica, Universitat de Lleida (UdL). Av. Rovira Roure, 177. E-25198 LLEIDA (Catalonia, SPAIN).

Josep Lluís GARCÉS[c], Francesc MAS[c]

[c] Departament de Química Física.
C/ Martí i Franquès, 1. E-08028 BARCELONA (Catalonia, SPAIN).

* corresponding author

Abstract

In order to enable a wider use of voltammetric methods in speciation analysis, it is convenient not to be restricted by ligand excess conditions. This work assumes labile ideal complexation of a metal ion by a ligand, planar electrode, no electrodic adsorption and equal diffusion coefficients for the complex and the ligand, but very different from the metal ion. It is shown that the system of non-linear equations describing the diffusion of the species in a potentiostatic experiment for any ligand to metal ratio can be reduced to only one ordinary differential equation by means of a change of variable. Standard numerical methods can then be used in the computation of the solution with a

Published in Journal of Electroanalytical Chemistry 1999, vol 472, p 42-52
doi:10.1016/S0022-0728(99)00259-4 reprints to galceran@quimica.udl.cat

great saving of computational time and resources in comparison with other existing methods. Some properties of the currents are also proved: i) cottrellian behaviour for any current in normal pulse polarography (NPP) and for limiting currents in reverse pulse polarography (RPP), ii) the dependence of the normalised limiting current (ϕ) on just 3 parameters and iii) the equality of limiting NPP and RPP currents. The normalised current for high stability constant values depend on just 2 parameters, one of which is the ratio of total metal / total ligand concentrations, and can be found from an implicit algebraic equation. A new representation for the normalised limiting currents is suggested: the iso-ϕ diagram, which for each ratio of diffusion coefficients, ε , describes the currents for any stability constant in a unique drawing. A new graphical procedure arising from this diagram is suggested and then applied to data corresponding to Zn / poly(methacrylic) acid at pH=6 and fixed ionic strength .

Keywords: voltammetry, macromolecular complexation, speciation, non-linear diffusion, pulse polarography, stability constant, concentration profiles.

1. Introduction

Voltammetric measurements are widely used in the speciation studies of systems containing macromolecules and metal ions, the major advantages being the reduced perturbation of the natural sample by the analytical procedure and the low detection limit of these techniques [1]. Both the shift of the half wave potential or the decrease of the limiting current can be suitable to obtain the stability constants. However, the determination of the binding curves from voltammetric data encounters some difficulties, among which the indirect determination of the free metal ions

Published in Journal of Electroanalytical Chemistry 1999, vol 472, p 42-52
doi:10.1016/S0022-0728(99)00259-4 reprints to galceran@quimica.udl.cat

concentration, the presence of transport steps and adsorption phenomena onto the electrode surface have been reported [2-4].

Up to now, most of the work concerning complexation has been done using a large excess of ligand [2,5] [6], because of the linearization of the problem. Recently, it has been pointed out that in excess ligand conditions any complexation model behaves like the ideal complexation model characterised by identical and independent sites (occupation or vacancy of one site does not affect the affinity of any other site) [4,7,7]. This supports the interpretation of ligand excess experimental results assuming ideal complexation for any system. The stability constant so obtained corresponds to an average of the intrinsic affinities of the sites. However, many other models of complexation can arise: intrinsically different sites (heterogeneity), chelates, lateral interactions,... and one must move away from the excess ligand conditions if any specific characteristic of the model has to be found. Thus, to deal with non-ideal complexation cases or to improve the determination of K in the ideal case, it is convenient to study the voltammetric responses beyond the ligand excess framework.

For any metal-to-ligand ratio, a non-linear system of equations arising from the transport of the metal (M), ligand (L) and complex (ML) has to be solved [4,8-10]. A finite difference scheme was used to compute the limiting current in a general case in which the kinetics of the complexation process are not sufficiently fast to reach quasi-equilibrium [11]. In this case, the effect of unfulfilment of lability on the titration curves has also been assessed [12]. When fully labile conditions are assumed, an equilibrium relationship for the concentrations of the formal species M, ML, and L can be written and the system can be reformulated in terms of only three differential equations,

Published in Journal of Electroanalytical Chemistry 1999, vol 472, p 42-52
doi:10.1016/S0022-0728(99)00259-4 reprints to galceran@quimica.udl.cat

corresponding to the total metal, the total ligand and the reduced metal, plus the algebraic equation coming from the equilibrium relationship that arises from full lability. Although finite difference schemes are applicable in this case, finite element methods (FEM) have also been applied [8,10,13], the major advantage of these latter techniques in the present problem being the natural use of unequal spatial grids, adapted to the physical viewpoint of the problem.

Recently, a discussion of the effects of ligand and complex adsorption on the limiting currents of the pulse polarographic techniques has been published [10]. For labile systems, no influence on the limiting RPP current can be found from complex adsorption, and if the ligand concentration is chosen for maximum sensitivity, the remaining effect of the ligand adsorption in limiting RPP currents leads to a bias in the stability constant, determined from the limiting current at zero metal concentration, less than 14%, provided that the complex and ligand are 20-fold slower than the metal. Moreover, for the case without adsorption, reference [10] suggests that limiting NPP currents do not differ from limiting RPP currents. So, the simpler expressions developed for NPP limiting currents can be used for the interpretation of results obtained from both techniques, even in systems with adsorption phenomena provided that limiting RPP currents are recorded.

The aim of this work is to point out that, for any ligand to metal ratio in labile metal-macromolecular complexation, the current produced in a potentiostatic step (e.g. direct current or dc polarography) can be obtained via a change of variables that transforms the partial differential equation into an ordinary differential equation (ODE). The process of reformulation of the original problem together with requirements for the

Published in Journal of Electroanalytical Chemistry 1999, vol 472, p 42-52
doi:10.1016/S0022-0728(99)00259-4
reprints to galceran@quimica.udl.cat

change to be valid are presented in section 3. The solution of the resulting equation requires much less computational effort and can be obtained using standard numerical methods, such as those based on Runge-Kutta algorithms. A practical implementation of the calculations needed is described in section 4. Taking advantage of this formulation, some general properties of the pulse polarographic currents are also deduced in section 5, proving, in particular, that $I_{lim,RPP} = I_{lim,NPP}$. Finally, these properties lead to the introduction, in section 6, of a new representation of the results, labelled as the iso-ϕ diagram. For a given ratio of diffusion coefficients ε, this diagram describes the (limiting) normalised currents for any stability constant in a unique drawing. A graphical procedure to estimate the stability constant from the iso-ϕ diagram is presented in section 7 and tested with experimental data from Zn / poly(methacrylic) acid.

2. Mathematical formulation

Let us consider the simple binding scheme in which an electroactive metal ion (M) forms a complex (ML) with a ligand (L) . When complexation and electron transfer kinetics are fast enough, equilibrium relationships for both the homogeneous reaction and the heterogeneous electron transfer processes can be assumed. This problem can be depicted as

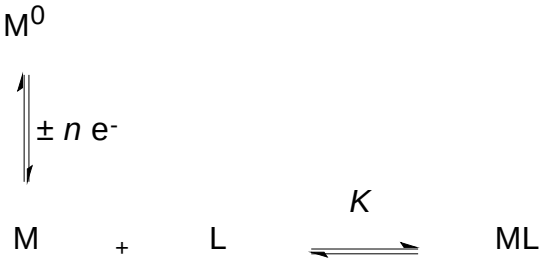

(1)

with K being the stability constant for the complexation reaction

Published in Journal of Electroanalytical Chemistry 1999, vol 472, p 42-52
doi:10.1016/S0022-0728(99)00259-4
reprints to galceran@quimica.udl.cat

$$K = c_{\mathrm{ML}} / \left(c_{\mathrm{M}}\, c_{\mathrm{L}} \right) \tag{2}$$

The assumption of instantaneous adaptation of c_{ML} to the equilibrium relationship is known as fully labile behaviour and allows a gradient of ML to develop close to the electrode when a step is applied. We assume that the diffusion coefficient for the metal in solution (D_{M}) is much greater than the diffusion coefficient for the complex or the ligand, whose common value is labelled D_{L}

Scheme (1) can also be seen as the reduced formulation [7,14] of a fully labile macromolecular system, with all the macromolecular species having the same fixed number of independent and homogeneous sites and the same diffusion coefficient [15]. In this case, c_{ML} is the concentration of bound metal, c_{L} the concentration of free sites and D_{L} is the diffusion coefficient of any macromolecular species.

When there is neither complex nor ligand adsorption and L and ML have the same diffusion coefficient, it can be seen [10,11] that, irrespective of the technique,

$$c_{\mathrm{T,L}}(x,t) \equiv c_{\mathrm{L}}(x,t) + c_{\mathrm{ML}}(x,t) = c_{\mathrm{L}}^{*} + c_{\mathrm{ML}}^{*} = c_{\mathrm{T,L}}^{*} \tag{3}$$

(where the asterisk superscript denotes bulk concentrations) since boundary conditions are fulfilled by the initial distribution of total ligand concentration and, at no time, there is any physical phenomenon modifying the total ligand concentration at any point.

Assuming planar symmetry, the total metal diffusion can be written as

$$\frac{\partial c_{\mathrm{M}}(x,t)}{\partial t} + \frac{\partial c_{\mathrm{ML}}(x,t)}{\partial t} = D_{\mathrm{M}} \frac{\partial^2 c_{\mathrm{M}}(x,t)}{\partial x^2} + D_{\mathrm{L}} \frac{\partial^2 c_{\mathrm{ML}}(x,t)}{\partial x^2} \tag{4}$$

Published in Journal of Electroanalytical Chemistry 1999, vol 472, p 42-52
doi:10.1016/S0022-0728(99)00259-4

and the diffusion of the reduced metal M^0 (either inside the amalgam or away from it, which is irrelevant in planar geometry) as

$$\frac{\partial c_{M^0}(x,t)}{\partial t} = D_{M^0} \frac{\partial^2 c_{M^0}(x,t)}{\partial x^2} \tag{5}$$

The initial conditions are given by:

$$c_M(x,0) = c_M^* \;;\; c_{ML}(x,0) = c_{ML}^* \quad ; \quad c_{M^0}(x,0) = 0 \qquad \forall x > 0 \tag{6}$$

and the boundary value problem, given by semi-infinite diffusion, reads

$$c_M(x,t) = c_M^* \;;\; c_{ML}(x,t) = c_{ML}^* \quad ; \quad c_{M^0}(x,t) = 0 \qquad \forall t > 0 \quad x \to \infty \tag{7}$$

and for $x = 0$,

$$D_M\left(\frac{\partial c_M}{\partial x}\right)_{x=0} + D_L\left(\frac{\partial c_{ML}}{\partial x}\right)_{x=0} + D_{M^0}\left(\frac{\partial c_{M^0}}{\partial x}\right)_{x=0} = 0 \tag{8}$$

and

$$\frac{c_{M^0}(0,t)}{c_M(0,t)} = \exp\left[-\frac{nF}{RT}\left(E - E^0\right)\right] \equiv \delta\sqrt{\frac{D_M}{D_{M^0}}} \tag{9}$$

arising respectively from a metal flux balance and from the electrochemical reversibility. Notice that the inclusion of $\sqrt{D_M/D_{M^0}}$ in the definition of δ is convenient for the planar electrode and other functionalities could arise in other geometries.

Equations (2)-(9) determine the four unknowns c_M, c_L, c_{ML} and c_{M^0}. In previous work [4,8,10,13,16,17] dealing with several pulse polarographic techniques, we have solved numerically the system of equations (2)-(9) using the Galerkin finite element method [18]. Here, we adopt a very different approach.

Published in Journal of Electroanalytical Chemistry 1999, vol 472, p 42-52
doi:10.1016/S0022-0728(99)00259-4

3. Transformation of the non-linear system of diffusion equations

Through the similarity method [19,20], a new variable

$$z \equiv x \Big/ \sqrt{D_{\mathrm{M}}\, t} \tag{10}$$

is introduced. This kind of change of variable is typical in the solution of non-uniform diffusion coefficients [21] and has also been used in the electrochemical field [22,23]. The inclusion of the constant value D_{M} is convenient in order to render z a dimentionless magnitude, which can be then thought as a normalised distance to the planar electrode. Using this new variable, equation (5) rewrites as

$$\frac{z}{2}\frac{\mathrm{d}\, c_{\mathrm{M}^0}(z)}{\mathrm{d}\, z} + \frac{D_{\mathrm{M}^0}}{D_{\mathrm{M}}}\frac{\mathrm{d}^2\, c_{\mathrm{M}^0}(z)}{\mathrm{d}\, z^2} = 0 \tag{11}$$

and equation (4) becomes

$$\frac{z}{2}\left(\frac{\mathrm{d}\, c_{\mathrm{M}}(z)}{\mathrm{d}\, z} + \frac{\mathrm{d}\, c_{\mathrm{ML}}(z)}{\mathrm{d}\, z}\right) + \frac{\mathrm{d}^2\, c_{\mathrm{M}}(z)}{\mathrm{d}\, z^2} + \varepsilon\frac{\mathrm{d}^2\, c_{\mathrm{ML}}(z)}{\mathrm{d}\, z^2} = 0 \tag{12}$$

where $\varepsilon \equiv D_{\mathrm{L}} / D_{\mathrm{M}}$.

Both equations (11) and (12) are ordinary differential equations in terms of z. We turn now our interest to their boundary value problem. Initial and boundary conditions at $x \to \infty$ reduce (without conflict) to only one condition at $z \to \infty$ when using the new variable z:

$$c_{\mathrm{M}}(z) = c_{\mathrm{M}}^{*} \qquad c_{\mathrm{ML}}(z) = c_{\mathrm{ML}}^{*} \qquad c_{\mathrm{M}^0}(z) = 0 \qquad z \to \infty \tag{13}$$

The boundary conditions at $x = 0$, now $z = 0$, become

Published in Journal of Electroanalytical Chemistry 1999, vol 472, p 42-52
doi:10.1016/S0022-0728(99)00259-4

$$D_{\mathrm{M}}\left(\frac{\mathrm{d}\,c_{\mathrm{M}}}{\mathrm{d}\,z}\right)_{z=0}+D_{\mathrm{L}}\left(\frac{\mathrm{d}\,c_{\mathrm{ML}}}{\mathrm{d}\,z}\right)_{z=0}+D_{\mathrm{M}^0}\left(\frac{\mathrm{d}\,c_{\mathrm{M}^0}}{\mathrm{d}\,z}\right)_{z=0}=0 \tag{14}$$

$$c_{\mathrm{M}^0}(0)=\delta\sqrt{\frac{D_{\mathrm{M}}}{D_{\mathrm{M}^0}}}\,c_{\mathrm{M}}(0) \tag{15}$$

Equations (11)-(15) determine the unknown functions $c_{\mathrm{M}}(z)$, $c_{\mathrm{ML}}(z)$ and $c_{\mathrm{M}^0}(z)$. Thus, the original system (given by eqns. (2)-(9)) has been successfully re-formulated using only the z variable provided that δ is kept constant (dc experiment), thus indicating that the spatial and time dependence of the unknowns is reduced to a combined dependence on $x/\sqrt{t}$. This reduction results in a great advantage in saving time and resources in the numerical computation of the solution of the system.

Another consequence of this combined dependence is the time independent value reached by the concentrations at the electrode surface for a given constant potential. In effect, as the concentrations depend only on z, and, as z does not change with time for x =0, concentrations at the electrode surface cannot be dependent on time during a dc experiment. Then, eqn. (11) can be straightforwardly integrated leading to the typical erfc functional dependence for the concentration profile of M^0 (see page 161 in ref. [24]).

Moreover, the profile of c_{M} in terms of z summarises any profile in terms of x at any time, i.e., any profile of the metal at any time collapses, by means of the change of variable, into this unique profile c_{M} vs. z which can be seen as the profile in terms of x at t = 1s. The collapse of the metal profiles (obtained via FEM calculation under limit

Published in Journal of Electroanalytical Chemistry 1999, vol 472, p 42-52
doi:10.1016/S0022-0728(99)00259-4

diffusion conditions) for different times and spatial positions into a unique profile is illustrated in Fig. 1. This correspondence of profiles also holds for any other species.

Through the equilibrium relationship (2) and equation (3), c_{ML} can be written in terms of c_M . Then, the only remaining differential equation (12) can be expressed in terms of only one unknown, such as c_M. But, for purposes that will be seen below, it is convenient to consider the product $K c_M(z)$ as the unknown function. Multiplying (12) by K, one obtains

$$\frac{z}{2}\frac{\mathrm{d}}{\mathrm{d}z}\left(K c_M - \frac{K c^*_{T,L}}{1+K c_M}\right) + \frac{\mathrm{d}^2}{\mathrm{d}z^2}\left(K c_M - \varepsilon\frac{K c^*_{T,L}}{1+K c_M}\right) = 0 \qquad (16)$$

The bulk boundary condition (13) and the initial condition (6) become

$$K c_M(z) = K c^*_M \qquad z \to \infty \qquad (17)$$

Recast in terms of $K c_M$ and z , the remaining boundary condition (14) becomes

$$\left(\frac{\mathrm{d}(K c_M)}{\mathrm{d}z}\right)_{z=0} = \frac{\delta}{1+\dfrac{\varepsilon K c^*_{T,L}}{\left(1+K c_M(0)\right)^2}}\frac{D_M}{\sqrt{\pi}\,D_{M^0}} K c_M(0) \qquad (18)$$

where (15) has been used.

Thus, the problem has been reduced to solving just the non-linear ordinary differential equation (16) subject to the boundary conditions (17) and (18). Once $K c_M(z)$ is known, any other characteristic of the system can be computed, such as the concentration profiles or the current. In the latter case, we write the x-gradients of c_{ML} and c_M in terms of the z-gradients of $K c_M(z)$, and finally obtain:

Published in Journal of Electroanalytical Chemistry 1999, vol 472, p 42-52
doi:10.1016/S0022-0728(99)00259-4

$$I(t) = n\,F\,A\left\{ D_{\mathrm{M}}\left(\frac{\partial c_{\mathrm{M}}}{\partial x}\right)_{x=0} + D_{\mathrm{L}}\left(\frac{\partial c_{\mathrm{ML}}}{\partial x}\right)_{x=0}\right\} = \frac{n\,F\,A\left(D_{\mathrm{M}} + \dfrac{D_{\mathrm{L}}\,K\,c^{*}_{\mathrm{T,L}}}{\left(1+K\,c_{\mathrm{M}}(0)\right)^{2}}\right)}{K\sqrt{D_{\mathrm{M}}t}}\left(\frac{\mathrm{d}(K\,c_{\mathrm{M}})}{\mathrm{d}\,z}\right)_{z=0} \tag{19}$$

One necessary condition for re-writing the differential equation in terms of just the new variable is that the boundary conditions cannot be time dependent (see ref. [21], page 38). For instance, adsorption processes at the electrode will generally prevent such change, one obvious exception being such a strong adsorption that the concentration of the adsorbate at the electrode falls to zero permanently. In the framework of the present work, the requirement of time independent boundary conditions means that δ in (15) is kept constant along the experiment, as in dc polarography, where there is only one step potential applied to each drop. However, since in the NPP technique (with no adsorption) there is no faradaic current during the first step ($0 \le t < t_0$), the initial uniform profile is not distorted, $c_{\mathrm{M}}(x, t < t_0) = c^{*}_{\mathrm{M}}$, the system behaves equivalently to the dc experiment with just a shift in time by t_0, and so the change of variable is valid. In other pulse polarographic techniques (such as DPP), the change of variables will be possible only during the first pulse. Usually this is the longest interval, lasting almost all drop life, so a great saving of computing time and resources will be obtained if this change of variables is used for the first period. Finite differences or finite element methods could then be used for the rest of time.

Published in Journal of Electroanalytical Chemistry 1999, vol 472, p 42-52
doi:10.1016/S0022-0728(99)00259-4

4. Numerical solution

Among the methods available to perform a numerical integration of an ODE, we have used a shooting method [25] to solve equation (16) with boundary conditions (17) and (18).

The calculation starts by introducing a first trial for $K\ c_M(0)$, which is used to find, through (18), the corresponding trial for the gradient of $K\ c_M(z)$ at z=0. With both trial values, numerical integration of (16) with a Runge-Kutta algorithm allows us to compute $K\ c_M(z \rightarrow \infty)$ which is compared with $K c_M^*$ and allows us to correct the previous trial for $K\ c_M(0)$. The procedure is repeated until the required accuracy is obtained.

As an example, an NPP wave obtained using this method is plotted in Fig. 2. The typical behaviour corresponding to excess of metal is observed: the first wave which develops around E_0 corresponds to the reduction of free metal before a noticeable reduction of the complex (through the instantaneous dissociation assumed in eqn. (2)) takes place. A detailed discussion of NPP and RPP waves obtained for any ligand to metal ratio with the finite element method is given elsewhere [8,10].

5. Properties

5.1 The current is cottrellian

The values of c_M and its x-gradient, at a given x, depend on t (see Fig. 1a). However, the value of c_M and its z-gradient, at a given z, is unique (see Fig. 1b). If $x = 0$, it follows that $z = 0$ regardless of the time and, so, there are unique values for c_M and its

Published in Journal of Electroanalytical Chemistry 1999, vol 472, p 42-52
doi:10.1016/S0022-0728(99)00259-4

z-gradient at *z*=0. Thus, equation (19) proves that the current has cottrellian behaviour (i.e. depends on time as $t^{-1/2}$), which is equivalent to the property given in page 37 of reference [21].

5.2 ϕ_{dc} and ϕ_{NPP} depend on $K c^*_{T,M}$, $K c^*_{T,L}$, ε and δ.

The normalised current ϕ [2] can be obtained dividing (19) by the current obtained when there is only metal[24]. We have,

$$\phi_{dc} = \phi_{NPP} \equiv \frac{\delta}{(1+\delta)} \frac{I(t_d)}{n F A c^*_{T,M}} \sqrt{\frac{\pi t_p}{D_M}} = \frac{\delta\sqrt{\pi}}{(1+\delta)} \frac{\left(1+\dfrac{\varepsilon K c^*_{T,L}}{\left(1+K c_M(0)\right)^2}\right)}{K c^*_{T,M}} \left(\frac{d(K c_M)}{d z}\right)_{z=0} \qquad (20)$$

where δ, given by equation (9), depends on the potential *E* applied during the pulse and $c_{T,M}$ stands for the total metal concentration $c_{T,M} \equiv c_M + c_{ML}$. Notice that, upon normalisation, the cottrellian time-dependence has cancelled out.:

Moreover, $K c_M(z)$ and its *z*-gradient at *z*=0, depend on the parameters affecting the differential equation (16) and its boundary conditions (17) and (18). It is clear that in (16) and (17), the parameters *K*, $c^*_{T,M}$ and $c^*_{T,L}$ do not appear separately but always as the products $K c^*_{T,M}$ and $K c^*_{T,L}$. If we turn to the boundary condition (17), putting $K c^*_M$ in terms of the products $K c^*_{T,M}$ and $K c^*_{T,L}$:

$$K c_M(z) = K c^*_M = \qquad z \to \infty$$
$$= \frac{-1 - K c^*_{T,L} + K c^*_{T,M} + \sqrt{\left(1 + K c^*_{T,L} - K c^*_{T,M}\right)^2 + 4 K c^*_{T,M}}}{2} \qquad (21)$$

Published in Journal of Electroanalytical Chemistry 1999, vol 472, p 42-52
doi:10.1016/S0022-0728(99)00259-4

we see that the combined dependence on $K c^*_{T,M}$ and $K c^*_{T,L}$ also holds. Thus we can ensure that $K c_M(z)$ and its gradient at z=0 depend on $K c^*_{T,M}$, $K c^*_{T,L}$, ε and δ. And, as no new parameters appear in (20), we can conclude $\phi_{dc} = \phi_{dc}\left(K c^*_{T,M}, K c^*_{T,L}, \varepsilon, \delta\right)$ and $\phi_{NPP} = \phi_{NPP}\left(K c^*_{T,M}, K c^*_{T,L}, \varepsilon, \delta\right)$.

5.3 Limiting NPP current

The limiting NPP current can be deduced as a particular case of the general framework developed above by restricting ourselves to the case where the potential becomes so negative that the arrival of M to the electrode is diffusion limited $c_M(0, t > t_0) = c_{ML}(0, t > t_0) = 0$. Thus, the only difference in the solution of (16) is the simplified form of the boundary condition replacing (18), which now reads $K c_M(0) = 0$ and, so, the previous properties hold:

i) The limiting current is cottrellian

ii) $\phi_{lim,NPP} = \phi_{lim,NPP}\left(K c^*_{T,M}, K c^*_{T,L}, \varepsilon\right)$. In particular, eqn. (20) becomes

$$\phi_{lim,dc} = \phi_{lim,NPP} = \frac{\sqrt{\pi}\left(1 + \varepsilon K c^*_{T,L}\right)}{K c^*_{T,M}} \left(\frac{d\left(K c_M\right)}{d z}\right)_{z=0} \qquad (22)$$

5.4 $I_{lim,NPP} = I_{lim,RPP}$

The equality of the limiting NPP and RPP currents is a well known result for a single diffusing electroactive species (or equivalent systems such as the excess ligand conditions) in planar geometry [24]. But the equality might not hold in other conditions. For instance, it is also well known that the equality does not hold in spherical geometry (see [26] and references therein) or in the presence of adsorption [10,27].

Published in Journal of Electroanalytical Chemistry 1999, vol 472, p 42-52
doi:10.1016/S0022-0728(99)00259-4

Now, we aim to prove the identical value of limiting RPP and NPP currents for the case analysed in this work: planar geometry, no adsorption and labile complexation with any ligand-to-metal ratio. For NPP without adsorption, the system does not evolve until the pulse application; so we need to consider just the second step as if it were the only one. The current can be written in terms of the *z*-gradient of M^0 and, then, expressed in terms of the concentration of c_{M^0} at the electrode surface:

$$I_{\mathrm{lim,NPP}}(t_\mathrm{d}) = -nFAD_{M^0}\left(\frac{\partial c_{M^0}}{\partial x}\right)_{x=0} = -nFA\frac{D_{M^0}}{\sqrt{D_M t_\mathrm{p}}}\left(\frac{\partial c_{M^0}}{\partial z}\right)_{z=0} = nFA\sqrt{\frac{D_{M^0}}{\pi t_\mathrm{p}}}c_{M^0}(0) \qquad (23)$$

because only the pulse time t_p is relevant in the NPP expression (without adsorption). We point out that $c_{M^0}(0)$ could be written as $c_{M^0}(0, t > t_0)$ which is a constant during the application of this step producing diffusion limited conditions.

In RPP, the electrode is held at a base potential in the diffusion limited region of the reactant, $c_M(0, t < t_0) = 0$ and, at $t = t_0$, pulses are applied to reverse the electrochemical reaction. To measure the limiting current, $I_{\mathrm{lim,RPP}}$, at least 2 drops are needed [28]. One of them, held at extremely negative potential during the drop time t_d, allows the determination of I_dc. The application of the diffusion limited potential step, according to what we have shown in (23), yields

$$I_\mathrm{dc}(t_\mathrm{d}) = nFA\sqrt{\frac{D_{M^0}}{\pi t_\mathrm{d}}}c_{M^0}(0) \qquad (24)$$

In another drop, to measure I_RP, the first potential step is extremely negative. During its application ($0<t<t_0$), the typical erfc functional dependence for c_{M^0} holds. At $t=t_0$, as we seek to measure the limiting RPP current, an extremely positive value of *E*

Published in Journal of Electroanalytical Chemistry 1999, vol 472, p 42-52
doi:10.1016/S0022-0728(99)00259-4

with respect to E_0 is applied. Thus, $c_{M^0}(x, t > t_0) = 0$. The linear nature of the diffusion eqn (5) for the product M^0 allows the treatment of the second step (during the pulse time t_p) with the superposition principle (see page 178 in ref. [24]). The corresponding current is

$$I_{RP}(t_d) = -nFA\sqrt{\frac{D_{M^0}}{\pi}}c_{M^0}(0, t < t_0)\left\{\frac{1}{\sqrt{t_d}} - \frac{1}{\sqrt{t_p}}\right\} \quad (25)$$

and so the limiting RPP current is

$$I_{lim,RPP}(t_d) = I_{RP}(t_d) - I_{dc}(t_d) = nFA\sqrt{\frac{D_{M^0}}{\pi}}c_{M^0}(0, t < t_0)\frac{1}{\sqrt{t_p}} \quad (26)$$

which equals the limiting NPP current (23) when noticing that $c_{M^0}(0, t<t_0)$, which is time independent, has the same value in both experiments and arises from a diffusion limited step on an undisturbed bulk profile.

An implication of the given equality of the limiting NPP and RPP currents is the cottrellian behaviour of $I_{lim,RPP}$ which leads to $\phi_{lim,RPP}$ being dependent on $Kc^*_{T,M}$, $Kc^*_{T,L}$ and ε, i.e. $\phi_{lim,RPP} = \phi_{lim,,RPP}\left(Kc^*_{T,M}, Kc^*_{T,L}, \varepsilon\right)$.

As the demonstration is based on the linearity of the diffusion equation of M^0 (5), the equality $I_{lim,NPP} = I_{lim,RPP}$ applies to any labile complexation model: heterogeneous, interaction between neighbouring sites, etc.

We highlight that, due to the restricted impact of adsorption on RPP limiting currents [10], the result obtained in this section suggests that one can estimate

Published in Journal of Electroanalytical Chemistry 1999, vol 472, p 42-52
doi:10.1016/S0022-0728(99)00259-4

parameters of the system measuring $I_{lim,RPP}$ and processing the data as if they were from $I_{lim,NPP}$ without adsorption.

6. Iso-ϕ diagrams

6.1 Definition

The reduced dependence of ϕ_{lim} (either in an NPP or RPP experiment) on just 3 parameters indicates the convenience of a new kind of representation, which could be called an "iso-ϕ diagram", where ε is a fixed constant and level curves for ϕ are reported in terms of the 2 remaining parameters in a contour plot. Although iso-ϕ diagrams could also be drawn with NPP currents for each fixed potential (i.e. δ) and ε, here we restrict ourselves to limiting currents to take advantage of the equality with limiting RPP currents.

Fig. 3 shows an iso-ϕ diagram for ε=0.0685, where points corresponding to different couples of [$\log(K\ c^*_{T,M})$, $\log(K\ c^*_{T,L})$]-values with the same ϕ-value are connected building up a level or contour curve. Representations with similar axis have been used to study properties (such as bulk average equilibrium constants) of ligand mixtures (see [29] and page 215 in ref. [1]). As $\sqrt{\varepsilon} \le \phi \le 1$, we know that the upper boundary of the diagram ($c^*_{T,L} \to \infty$) corresponds to the level curve $\phi = \sqrt{\varepsilon}$, while the lower and rightmost boundary of the diagram ($c^*_{T,L} \to 0$) corresponds to the level curve $\phi = 1$.

Published in Journal of Electroanalytical Chemistry 1999, vol 472, p 42-52
doi:10.1016/S0022-0728(99)00259-4

An iso-ϕ diagram gathers, for a fixed ε, all the information about the ϕ-values for any *K*. This information: a) has customarily been displayed as $\phi - c^*_{T,L}$ plots [2] and b) has recently been suggested to be shown in ϕ- $c^*_{T,M}$ plots [4,10].

a) A $\phi - c^*_{T,L}$ plot corresponds to a vertical line in an iso-ϕ diagram, as a fixed amount of metal is taken. When comparing two imaginary vertical lines drawn in the very low $c^*_{T,M}$ region, one finds no difference in the spacing between level curves crossed by both vertical lines, as expected from the known result that $\phi - c^*_{T,L}$ plots are $c^*_{T,M}$ independent in excess ligand conditions. If one of these vertical lines moves towards higher $c^*_{T,M}$ values, one notices a change in the spacing of the level curves, which indicates the unfulfilment of the excess ligand conditions. The higher $c^*_{T,M}$ (i.e. moving the vertical rightwards), the closer the level curves become at high enough $c^*_{T,L}$.

b) A ϕ- $c^*_{T,M}$ plot [4] corresponds to a horizontal line in an iso-ϕ diagram, as $c^*_{T,L}$ is fixed. The excess ligand zone can be easily recognised at the left region of the diagram ($c^*_{T,M} << c^*_{T,L}$) where the level curves are horizontal: no dependence of the normalised current is noticed with changes in $c^*_{T,M}$, as in excess conditions the well known expression

$$\phi = \sqrt{\frac{1 + \varepsilon K c^*_{T,L}}{1 + K c^*_{T,L}}} \qquad (27)$$

applies. As can be seen in Fig. 3, the transition of ϕ from the excess ligand value given by (27) to a nearly unity value is much sharper for an upper horizontal line

Published in Journal of Electroanalytical Chemistry 1999, vol 472, p 42-52
doi:10.1016/S0022-0728(99)00259-4

(corresponding to higher $c^*_{T,L}$) than for a lower one. Let us follow a horizontal line corresponding to an initial low concentration of $c^*_{T,M}$ which is successively increased. For low enough $c^*_{T,M}$ (left of the diagram) the level curves are practically flat and so our horizontal line simply follows the level curve: ϕ does not change with $c^*_{T,M}$ because we are in the excess ligand region. Progressively the level curves bend upwards, this implying that the horizontal line is crossing level curves corresponding to higher ϕ values. The unfulfilment of excess ligand conditions leads to actual currents greater than those predicted by excess conditions, which can be intuitively interpreted by noticing that the approximation underestimates the metal concentrations along the diffusion layer due to an overestimation of the free ligand concentration.

Let us follow a level curve starting from the left. First we find the flat region corresponding to ligand excess conditions. The level curve progressively is clearly seen to bend upwards when the amount of metal increases sufficiently. Here, excess ligand conditions begin to fail and each increase in $c^*_{T,M}$ must be balanced with another increase in $c^*_{T,L}$ in order to keep ϕ constant along the level curve that we are following. Eventually, the increases in both concentrations converge to keep a certain ratio, as can be seen in the upper right corner of Figs. 3 and 4: each level curve asymptotically tends to a straight line of unit slope (parallel to the diagonal of the diagram which is depicted in discontinuous line). This property is discussed in detail in sub-section 6.2.

Due to the logarithmic scale of both axis, each ratio $c^*_{T,M}/c^*_{T,L}$ corresponds to a line of unit slope (i.e. a parallel to the diagonal $c^*_{T,M}=c^*_{T,L}$) . A point representing the

Published in Journal of Electroanalytical Chemistry 1999, vol 472, p 42-52
doi:10.1016/S0022-0728(99)00259-4
reprints to galceran@quimica.udl.cat

system moves upwards and rightwards along this line when concentrating the sample and downwards and leftwards when diluting.

As pointed out above, there is an iso-ϕ diagram for each ε. Comparison of the diagram for ε=0.0685 (Fig. 3) and for ε=0.25 (Fig. 4) indicates that higher ε-values give rise to higher normalised currents for a given couple $[c^*_{T,M}, c^*_{T,L}]$ and, thus, the range of variation of ϕ is narrower although the global pattern of the level curves is the same.

6.2 The limit of high stability constants

Let us take fixed values for $c^*_{T,L}$ and $c^*_{T,M}$. As *K* increases, we move upwards and to the right in the iso-ϕ diagram (see Figs. 3 and 4). The limiting behaviour in the corner is described by letting *K* tend to infinity. If $c^*_{T,L} \geq c^*_{T,M}$ all the metal is in complexed form and

$$\lim_{\substack{K\to\infty \\ c^*_{T,M}<c^*_{T,L}}} \phi = \sqrt{\varepsilon} \qquad (28)$$

As said above, the level curve $\phi = \sqrt{\varepsilon}$ corresponds to the lowest possible value in the diagram (and "bounds" the upper region of the iso-ϕ diagram) and can be seen as the level curve that eventually (for infinite *K*) tends to the diagonal of the diagram ($c^*_{T,L} = c^*_{T,M}$, discontinuous line in the figures). This implies that all the practical level curves (i.e. for $\phi > \sqrt{\varepsilon}$) for high $K c^*_{T,L}$ and $K c^*_{T,M}$ values eventually lie below the diagonal (see the upper right region of Fig. 4) where $c^*_{T,M} > c^*_{T,L}$

Published in Journal of Electroanalytical Chemistry 1999, vol 472, p 42-52
doi:10.1016/S0022-0728(99)00259-4

So, in order to know which is the asymptotic limit of any level curve we must study the case $c^*_{T,M} > c^*_{T,L}$. We begin by noticing that, if K tends to infinity, either c_L or c_M must vanish in order to render (through the equilibrium relationship (2)) a finite value for c_{ML} which is bound by the finite value $c^*_{T,L}$. In Fig. 5 we can see the z-profiles of the 3 species for very high K (markers correspond to FEM simulation data). In the region close to the electrode, there is some ligand and no metal (since the latter is depleted to 0 on the electrode surface). This region ends at a normalised distance z_0 where both c_L and c_M tend to 0.

For $z<z_0$, the diffusion equation (12) collapses into

$$\frac{z}{2}\frac{\mathrm{d}c_{ML}}{\mathrm{d}z} + \varepsilon\frac{\mathrm{d}^2 c_{ML}}{\mathrm{d}z^2} = 0 \tag{29}$$

which corresponds to the diffusion of just complex. The solution of (29), with the appropriate boundary conditions, is

$$\frac{\mathrm{d}c_{ML}}{\mathrm{d}z} = \frac{c^*_{ML}}{\sqrt{\pi\varepsilon}\,\mathrm{erf}\left(\frac{z_0}{2\sqrt{\varepsilon}}\right)}\mathrm{e}^{-\frac{z^2}{4\varepsilon}} = \frac{\mathrm{d}c_{T,M}(z<z_0)}{\mathrm{d}z} \tag{30}$$

Analogously, for $z>z_0$ there is just metal diffusion, leading to

$$\frac{\mathrm{d}c_{M}}{\mathrm{d}z} = \frac{c^*_{M}}{\sqrt{\pi}\,\mathrm{erfc}\left(\frac{z_0}{2}\right)}\mathrm{e}^{-\frac{z^2}{4}} = \frac{\mathrm{d}c_{T,M}(z>z_0)}{\mathrm{d}z} \tag{31}$$

The normalised limiting current can be computed from (22) and (30) as

Published in Journal of Electroanalytical Chemistry 1999, vol 472, p 42-52
doi:10.1016/S0022-0728(99)00259-4

$$\phi = \frac{c^*_{\mathrm{T,L}}\sqrt{\varepsilon}}{c^*_{\mathrm{T,M}}\,\mathrm{erf}\left(\dfrac{z_0}{2\sqrt{\varepsilon}}\right)} \tag{32}$$

In order to find z_0, we notice that the continuity of $c_{\mathrm{T,M}}$ implies

$$D_L\left(\frac{\partial c_{ML}}{\partial z}\right)_{z_0^-} = D_M\left(\frac{\partial c_M}{\partial z}\right)_{z_0^+} \tag{33}$$

which, using (30) and (31), yields an algebraic condition for z_0 :

$$\frac{\sqrt{\varepsilon}\,e^{-\frac{z_0^2}{4\varepsilon}}}{\mathrm{erf}\left(\dfrac{z_0}{2\sqrt{\varepsilon}}\right)} = \left(\frac{c^*_{\mathrm{T,M}}}{c^*_{\mathrm{T,L}}} - 1\right)\frac{e^{-\frac{z_0^2}{4}}}{\mathrm{erfc}\left(\dfrac{z_0}{2}\right)} \tag{34}$$

Thus, for this case of infinite K, we just need to solve a non-linear algebraic equation instead of the ordinary differential equation.

We notice that z_0 depends on the ratio $c^*_{\mathrm{T,M}}/c^*_{\mathrm{T,L}}$ rather than on each separate value, and so (for K tending to infinity which corresponds to the upmost and rightmost side of the iso-ϕ diagram) $\phi = \phi\left(\varepsilon, c^*_{\mathrm{T,M}}/c^*_{\mathrm{T,L}}\right)$. Hence, we conclude that all the level curves tend asymptotically to a straight line parallel to the diagonal (i.e. $c^*_{\mathrm{T,M}}/c^*_{\mathrm{T,L}}$=constant or $\log(c^*_{\mathrm{T,L}}) = \log(c^*_{\mathrm{T,M}}) + \text{constant}$).

Thus, as no information on K (except for the knowledge of being very high) appears on the upper right zone of the diagram, if we find our system to be there, dilution could prove useful to shift the system to a K-sensitive region (see page 274 in ref. [1]).

Published in Journal of Electroanalytical Chemistry 1999, vol 472, p 42-52
doi:10.1016/S0022-0728(99)00259-4

7 Determination of K from experimental normalised currents. Application to the Zn-PMA system

The iso-ϕ diagrams allows us to suggest an easy graphical method to estimate the stability constant in labile metal-macromolecule complexation systems. Due to the choice of a logarithmic scale, an iso-ϕ diagram can also be used in systems where K is unknown; indeed, the property $\log\left(K\, c^*_{\mathrm{T,M}}\right) = \log(K) + \log\left(c^*_{\mathrm{T,M}}\right)$ implies that the pattern of the level curves does not change when the axis values are taken as $\log\left(c^*_{\mathrm{T,M}}\right)$ and $\log\left(c^*_{\mathrm{T,L}}\right)$ instead of $\log\left(K\, c^*_{\mathrm{T,M}}\right)$ and $\log\left(K\, c^*_{\mathrm{T,L}}\right)$. So, the only effect in changing K to 1 is a shift of all level curves by the amount log (K) both in abscissas and ordinates. Thus, the following graphical method could be useful in some cases. Once ε is known, an iso-ϕ diagram can be drawn. Let ϕ_{exp} be the experimental ϕ value for a couple $\left[c^*_{\mathrm{T,M\ exp}}, c^*_{\mathrm{T,L\ exp}}\right]$. The point with co-ordinates $\left[\log\left(c^*_{\mathrm{T,M\ exp}}\right), \log\left(c^*_{\mathrm{T,L\ exp}}\right)\right]$ in the iso-ϕ diagram will usually not lie on the level curve corresponding to the experimental value ϕ_{exp} unless K = 1. To quantify the shift due to the unknown K, one can draw a straight line of unity slope passing through the experimental point and then determine its intersection with the level curve $\phi = \phi_{\mathrm{exp}}$ in the iso-ϕ diagram. Either the horizontal or the vertical distance between the experimental point and the intercept with the level curve provides the value of the logarithm of K. There is freedom for the election of the units of the concentration, which then determines the units for K. Iso-ϕ diagrams for any ε (or software necessary to generate them) are available from the authors upon request.

Published in Journal of Electroanalytical Chemistry 1999, vol 472, p 42-52
doi:10.1016/S0022-0728(99)00259-4

This procedure has been applied to experimental results obtained from Zn-PMA (polymethacrylic acid) at 0.01 M KNO_3, corresponding to a titration of a solution of PMA with Zn, using the methodology, chemicals and apparatus of previous works [10]. The pH was kept close to 6 by convenient addition of 0.05M KOH solution, when necessary[30]. Fig. 6 shows an example of the application of this graphical method with the iso-ϕ diagram corresponding to ε = 0.06 (value given for Zn - PMA in ref. [10]). The experimental measurements recorded in Table 1 (marker - in Fig. 6)) exhibit a slight departure from the horizontality indicating the dilution effect. Positions for ϕ = 0.55, 0.60, 0.65 and 0.70 (markers ■ in Fig. 6) have been obtained through linear interpolation using the closest experimental values. From each of these interpolated points a straight line of unity slope has been drawn. Then, the intersection with the corresponding iso-ϕ level curve has been determined (intersection points are labelled A, B, C and D, respectively in Fig. 6 and in Table 2). The subtraction of the abscissas or the ordinates of these intersection points from the interpolated experimental points provides values for log (K) (which are summarised in Table 2). The average value, log (K/mM^{-1})=1.16±0.06, is in good agreement with previous results, log (K/mM^{-1})=1.20±0.02, where a different procedure was employed ([10]).

Instead of the graphical method (which furnishes a quick estimate of the log (K)) a numerical approach can be applied by fitting K in (16) so that the normalised current obtained with (22) (through the iterative method explained in section 4) reproduces ϕ_{exp}. By processing data contained in the 3 first columns of Table 1 (log ($c^*_{T,M}$), log ($c^*_{T,L}$) and ϕ_{exp}), we obtain for each row, a log K-value. Their average value also is log (K/mM^{-1})=1.16±0.06. If we compare the results of the graphical method and the numerical approach we can conclude that the first one is a quick and accurate method to determine

Published in Journal of Electroanalytical Chemistry 1999, vol 472, p 42-52
doi:10.1016/S0022-0728(99)00259-4

the *K*-value. Moreover, it must be pointed out that when the experimental ϕ-value increases, the iso-ϕ diagram warns us that the determination of the *K*-value becomes more inaccurate, because the iso-ϕ curve tends to be almost diagonal. In this case a small error in the location of the interpolated experimental iso-ϕ value leads to a far away intersection point due to the small difference in the slope of both intersecting lines: the target level curve and the line of unity slope passing through the experimental point $\left[\log\left(c^*_{\mathrm{T,M}}\right), \log\left(c^*_{\mathrm{T,L}}\right)\right]$. So this graphical method could also be useful for the experimental design in order to achieve good sensibility for *K*.

Conclusions

It has been shown that the spatial and time dependence of the concentration profiles in a dc experiment of an electrochemical reversible system with labile complexation for any ligand to metal ratio reduce to just a combined dependence in terms of $x/\sqrt{t}$ when homogeneous initial conditions and semi-infinite diffusion hold.

This combined dependence enables the use of a change of variables which transforms the partial differential equation that models the behaviour of the system into an ordinary differential equation allowing a great save of computational time in the calculation of the current. Standard numerical methods can then be used to compute the concentration profiles and the current, or alternatively, to fit the stability constant *K* from an experimental ϕ value.

Some general properties of the dc currents have also been pointed out:

– cottrellian ($t^{1/2}$) time-dependence of the current.

Published in Journal of Electroanalytical Chemistry 1999, vol 472, p 42-52
doi:10.1016/S0022-0728(99)00259-4

- dependence of the current on just 4 parameters for a fixed time: $Kc^*_{T,M}$, $Kc^*_{T,L}$, D_L/D_M and E.
- time independence of the concentrations at the electrode surface.

Special attention has been devoted to the limiting currents. They depend, for a fixed time, on just $Kc^*_{T,M}$, $Kc^*_{T,L}$ and ε. This suggests the interest of a so-called iso-ϕ diagram (level curves for constant ϕ-values are plotted in terms of $Kc^*_{T,M}$ and $Kc^*_{T,L}$) which gathers all the information about the normalised limiting currents of the system (characterised by a given ε).

A graphical procedure to obtain the stability constant from an experimental measurement of the normalised (limiting) current for any ligand to metal ratio using the corresponding iso-ϕ diagram is suggested. Another practical application of this diagram is the assessment of the accuracy of the determination of K from a given couple of total ligand and metal concentrations. Illustration of this procedure for the Zn-PMA voltammetric currents is reported. The K-value obtained is in good agreement with values previously published.

All the properties above mentioned also hold for an NPP experiment without adsorption, since it reduces to a dc experiment lasting the pulse time (t_p). The equality $I_{lim,NPP} = I_{lim,RPP}$ has been proved for any ligand to metal ratio under planar geometry and no adsorption, and, thus, the properties also apply for $I_{lim,RPP}$. This result and the reduced impact of adsorption in limiting RPP currents suggest the use of RPP in cases where adsorption is present and allow the use of simpler expressions (derived for NPP

Published in Journal of Electroanalytical Chemistry 1999, vol 472, p 42-52
doi:10.1016/S0022-0728(99)00259-4

without adsorption) in the interpretation of the limiting RPP currents. The change of variables could also prove useful in the computation of the current in any impulsional technique, since it can be used during the first pulse time which usually corresponds to the longest interval.

Acknowledgements

The authors gratefully acknowledge support of this research by the Spanish Ministry of Education and Science (DGICYT: Project PB96-0379), from the "Ajuntament de Lleida" and from the "Comissionat d'Universitats i Recerca de la Generalitat de Catalunya". Finally, financial support from the "Generalitat de Catalunya" (FI grant for J.L. Garcés) and from the "Ministerio de Educación y Cultura" (FPI grant to E. Companys) is also acknowledged.

Published in Journal of Electroanalytical Chemistry 1999, vol 472, p 42-52
doi:10.1016/S0022-0728(99)00259-4

CAPTIONS FOR FIGURES

Fig. 1 Collapse of the profiles of metal concentration. a) profiles of normalised metal concentration at different times. b) the same normalised metal concentrations of a) but in terms of z. Parameters are: K=10^5 m^3 mol^{-1}; D_{M^0} =2 10^{-9} m^2 s^{-1}; D_M =7.3 10^{-10} m^2 s^{-1}; $D_{ML} = D_L$ =5 10^{-11} m^2 s^{-1}; $c^*_{T,M}$ =10 mol m^3; $c^*_{T,L}$ = 8 mol m^3; A=5.2 10^{-7} m^2; n=2; T=298.15 K; t_0=0.95 s; t_d=1 s; t= (◆) 0.02 s, (▲) 0.06 s, (○) 0.1 s, (+) 0.14 s, (–) 0.18 s, (◊) 0.2 s.

Fig. 2 NPP wave obtained through FEM calculation (markers) and through the change of variable combined with the shooting method (solid line). Parameters as in Fig 1.

Fig. 3 Iso-ϕ diagram obtained with ε=0.0685. The additional discontinuous line depicts the diagonal of the diagram ($c^*_{T,L} = c^*_{T,M}$).

Fig. 4 Iso-ϕ diagram obtained with ε=0.25.

Fig. 5 Concentration profiles of metal (marker Ý), complex (⇌) and ligand ( ) in terms of z as obtained from finite element simulation for parameters given in fig 1 at t=0.2 s. Depicted in solid lines, the same profiles from equations given in section 6.2 (arising from taking $K \to \infty$) .

Fig. 6 Graphical estimation of the stability constant with an iso-ϕ diagram from experimental data for Zn-PMA. The diagram has been drawn with ε=0.06. Marker - stands for the experimental points and marker (■) stands for the interpolated points of ϕ. The intersection between each discontinuous line (starting from the interpolated point and with unity slope) and the level curve having the same ϕ value as the interpolated point is shown with marker (Ý) and a capital letter (A, B, C or D).

Published in Journal of Electroanalytical Chemistry 1999, vol 472, p 42-52
doi:10.1016/S0022-0728(99)00259-4
reprints to galceran@quimica.udl.cat

Tables

Table 1 Experimental ϕ values and calculated stability constants obtained from RPP titrations for the Zn(II)/PMA system.[a]

$\log\left(c^{*}_{\mathrm{T,M}}/\mathrm{mM}\right)$	$\log\left(c^{*}_{\mathrm{T,L}}/\mathrm{mM}\right)$	ϕ_{exp}	$\log\left(K/\mathrm{mM}^{-1}\right)$ [b]
-1.706	-0.603	0.519	1.17
-1.406	-0.604	0.543	1.12
-1.231	-0.605	0.554	1.11
-1.107	-0.606	0.551	1.14
-1.011	-0.607	0.555	1.16
-0.933	-0.608	0.563	1.16
-0.867	-0.609	0.569	1.17
-0.810	-0.610	0.562	1.21
-0.715	-0.611	0.589	1.19
-0.638	-0.613	0.586	1.26
-0.572	-0.615	0.624	1.20
-0.516	-0.617	0.637	1.22
-0.467	-0.619	0.652	1.23
-0.423	-0.620	0.697	1.11
-0.383	-0.622	0.714	1.09
-0.347	-0.624	0.726	1.10
-0.314	-0.626	0.743	1.07

Published in Journal of Electroanalytical Chemistry 1999, vol 472, p 42-52
doi:10.1016/S0022-0728(99)00259-4
reprints to galceran@quimica.udl.cat

[a] Parameters used are: t_d = 0.8 s, t_p = 50 ms, A ⌒ 0.52 10^{-6} m^2, pH = 6 (adjusted for each titration point using 0.05 M KOH solution), ionic strength (KNO_3) = 0.01 M, T=25ºC.

[b] Fitted K-values from equations (16) and (22), as explained in section 4.

Table 2

Estimated log(K) values (graphical method, see Fig 6), using data given in table 1.

ϕ	coordinates $\left[\log(c^*_{T,M}/\text{mM}), \log(c^*_{T,L}/\text{mM})\right]$ of the interpolated point	coordinates $\left[\log(c^*_{T,M}/\text{mM}), \log(c^*_{T,L}/\text{mM})\right]$ of the intersection point	$\log(K / \text{mM}^{-1})$
0.55	[-1.292, -0.604]	A = [-0.18, 0.51]	1.11
0.60	[-0.614, -0.614]	B = [0.63, 0.63]	1.24
0.65	[-0.474, -0.618]	C = [0.76, 0.62]	1.24
0.70	[-0.416, -0.621]	D = [0.69, 0.48]	1.11

Published in Journal of Electroanalytical Chemistry 1999, vol 472, p 42-52
doi:10.1016/S0022-0728(99)00259-4

References

[1] J. Buffle, Complexation Reactions in Aquatic Systems. An Analytical Approach., Ellis Horwood Limited, Chichester, 1988, Chapter 9, p. 467.

[2] H.P. van Leeuwen, J. Buffle and R. Cleven, Pure Appl. Chem. 61 (1989) 255.

[3] A.M. Mota and M.M. Correia dos Santos, in A. Tessier and D. R. Turner (Eds.), Metal Speciation and Bioavailability in Aquatic Systems, John Wiley & Sons, Chichester, 1995,

[4] J.L. Garces, F. Mas, J. Cecilia, J. Galceran, J. Salvador and J. Puy, Analyst. 121 (1996) 1855.

[5] F. Mas, J. Puy, J.M. Diazcruz, M. Esteban and E. Casassas, J. Electroanal. Chem. 326 (1992) 299.

[6] J. Puy, F. Mas, J.M. Diazcruz, M. Esteban and E. Casassas, Anal. Chim. Acta 268 (1992) 261.

[7] J.L. Garces, F. Mas, J. Puy, J. Galceran and J. Salvador, J.Chem.Soc.Faraday Trans. 94 (1998) 2783.

[8] J. Puy, J. Galceran, J. Salvador, J. Cecilia, J.M. Diazcruz, M. Esteban and F. Mas, J. Electroanal. Chem. 374 (1994) 223.

[9] J.P. Pinheiro, A.M. Mota and M.L.S.S. Gonçalves, J. Electroanal. Chem. 402 (1996) 47.

Published in Journal of Electroanalytical Chemistry 1999, vol 472, p 42-52
doi:10.1016/S0022-0728(99)00259-4 reprints to galceran@quimica.udl.cat

[10] J. Puy, M. Torrent, J. Monne, J. Cecilia, J. Galceran, J. Salvador, J.L. Garces, F. Mas and F. Berbel, J. Electroanal. Chem. 457 (1998) 229.

[11] H.P. van Leeuwen, K. Holub and H.G. DeJong, J. Electroanal. Chem. 260 (1989) 213.

[12] M.R. Presa, J.A. Catoggio, D. Posadas and R.I. Tucceri, J. Electroanal. Chem. 432 (1997) 229.

[13] J. Cecilia, J. Galceran, J. Salvador, J. Puy and F. Mas, Int. J. Quantum Chem. 51 (1994) 357.

[14] J. Galceran, J. Salvador, J. Puy, F. Mas and H.P. van Leeuwen, J. Electroanal. Chem. 391 (1995) 29.

[15] H.P. van Leeuwen, Sci. Total Envir. 60 (1987) 45.

[16] J. Cecilia. Ph.D. Thesis. UPC, 1995.

[17] J. Galceran, J. Salvador, J. Puy, J. Cecilia, M. Esteban and F. Mas, Anal. Chim. Acta 305 (1995) 273.

[18] T.J.R. Hughes, The Finite Element Method, Prentice Hall, Englewood Cliffs,N.J., 1987.

[19] G. Bluman and S. Kumei, J. Math. Phys. 21 (1980) 1019.

[20] D. Zwillinger, Handbook of Differential Equations, Second ed. Academic Press, Boston MA, 1992.

[21] J. Crank, The Mathematics of Diffusion, 2nd ed. Clarendon Press, Oxford, 1975.

Published in Journal of Electroanalytical Chemistry 1999, vol 472, p 42-52
doi:10.1016/S0022-0728(99)00259-4

[22] K.B. Oldham, J. Electroanal. Chem. 122 (1981) 1.

[23] K.B. Oldham, J. Electroanal. Chem. 420 (1997) 53.

[24] A.J. Bard, L.R. Faulkner, Electrochemical Methods, Fundamentals and Applications, Wiley, New York, 1980.

[25] W.H. Press, B.P. Flannery, S.A. Teukolsky and W.T. Vetterling, Numerical Recipes, Cambridge University Press, Cambridge, 1986.

[26] J. Galceran, J. Salvador, J. Puy, F. Mas, D. Gimenez and M. Esteban, J. Electroanal. Chem. 442 (1998) 151.

[27] J. Galceran, D. Rene, J. Salvador, J. Puy, M. Esteban and F. Mas, J. Electroanal. Chem. 375 (1994) 307.

[28] J.G. Osteryoung and E. Kirowa-Eisner, Anal. Chem. 52 (1980) 62.

[29] P. MacCarthy and G.C. Smith, in B. A. Jenne (Ed.), Chemical Modeling in Aqueous Systems, ACS, Washington D.C., 1979, Chapter 10, p. 201.

[30] J.P. Pinheiro, A.M. Mota, M.L.S. Gonçalves and H.P. van Leeuwen, Environ. Sci. Technol. 28 (1994) 2112.

Published in Journal of Electroanalytical Chemistry 1999, vol 472, p 42-52
doi:10.1016/S0022-0728(99)00259-4 reprints to galceran@quimica.udl.cat

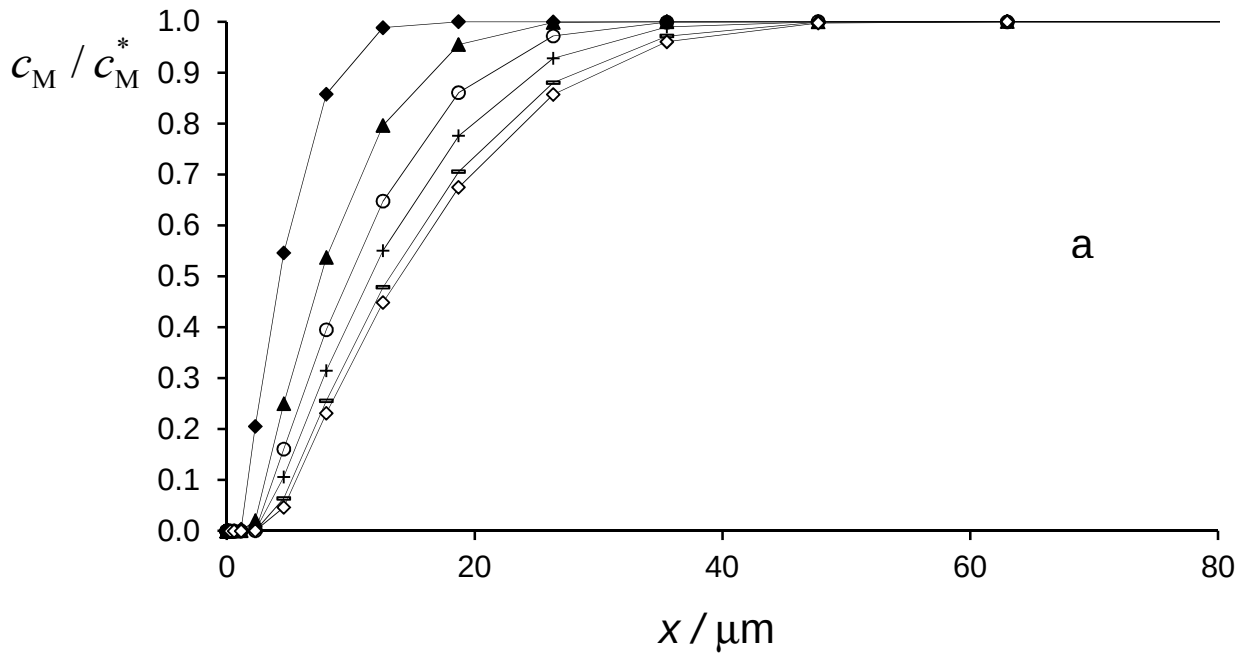

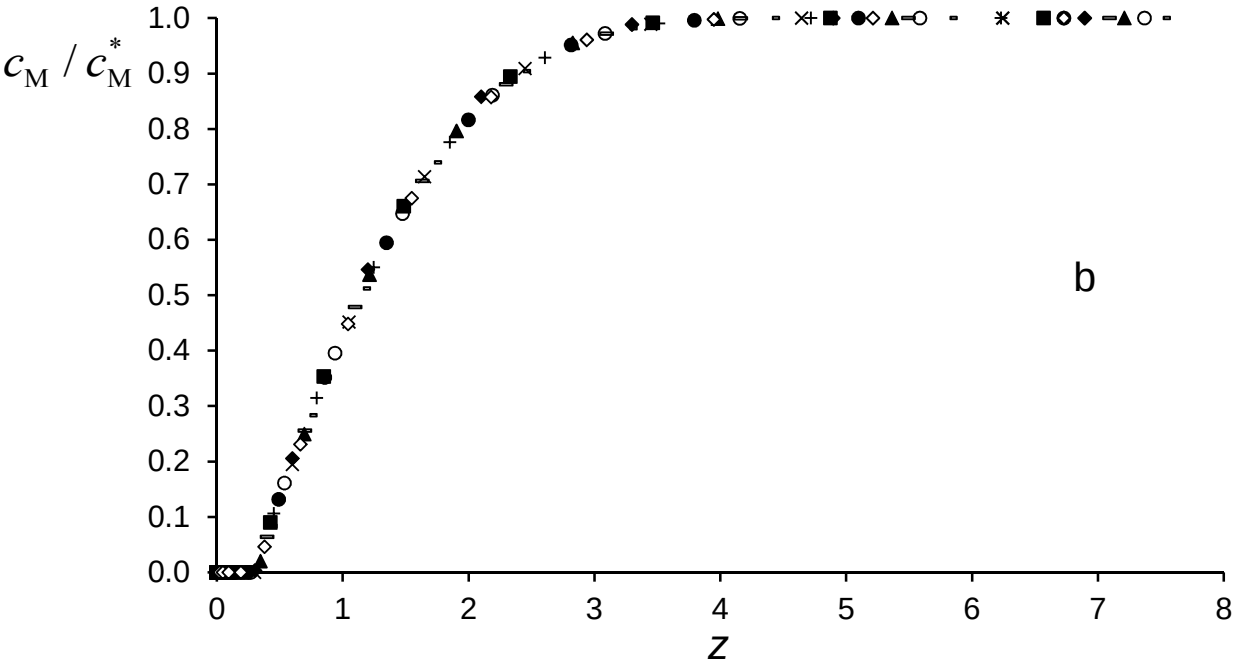

Fig 1

Published in Journal of Electroanalytical Chemistry 1999, vol 472, p 42-52
doi:10.1016/S0022-0728(99)00259-4
reprints to galceran@quimica.udl.cat

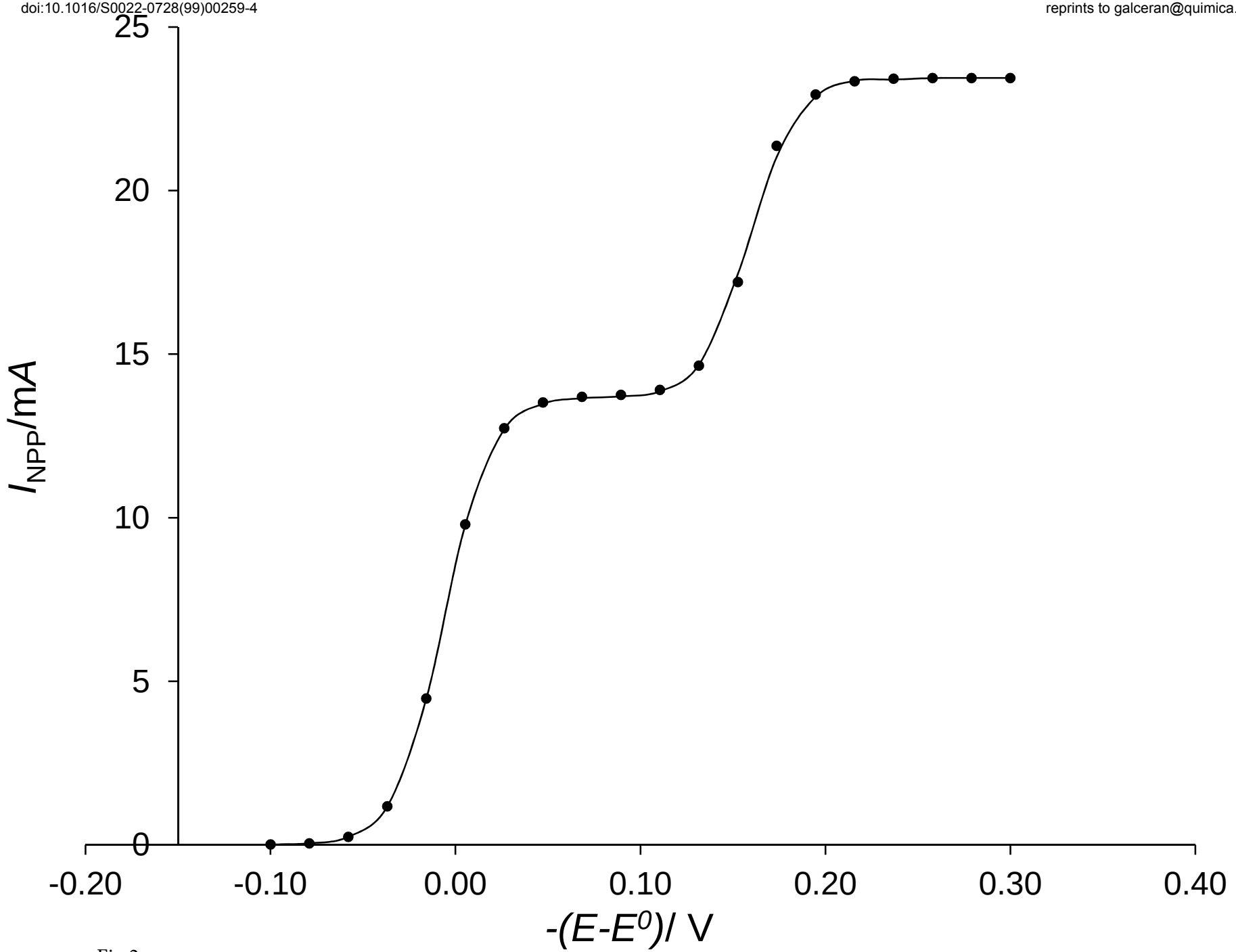

Fig 2

Published in Journal of Electroanalytical Chemistry 1999, vol 472, p 42-52
doi:10.1016/S0022-0728(99)00259-4
reprints to galceran@quimica.udl.cat

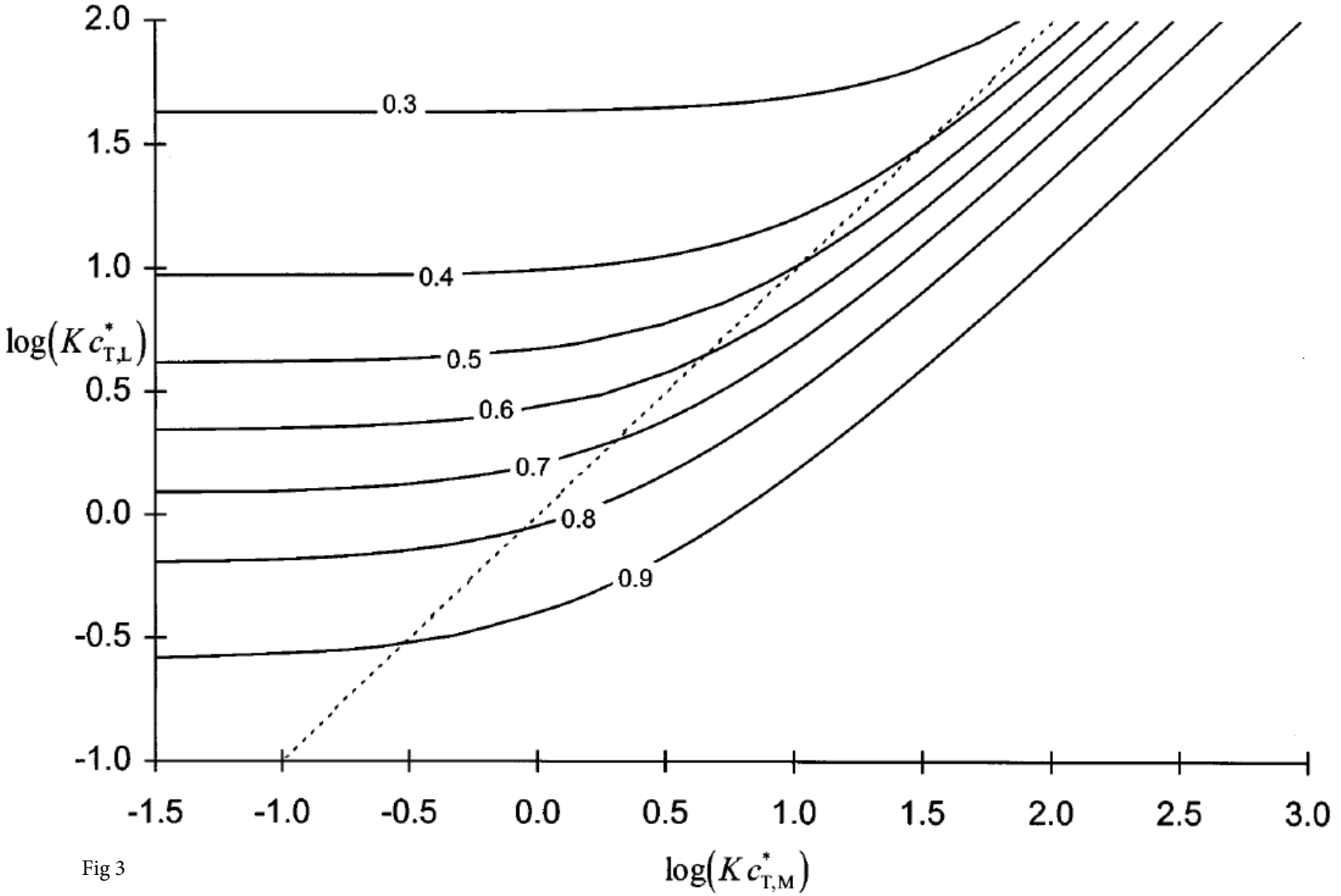

Fig 3

Published in Journal of Electroanalytical Chemistry 1999, vol 472, p 42-52
doi:10.1016/S0022-0728(99)00259-4

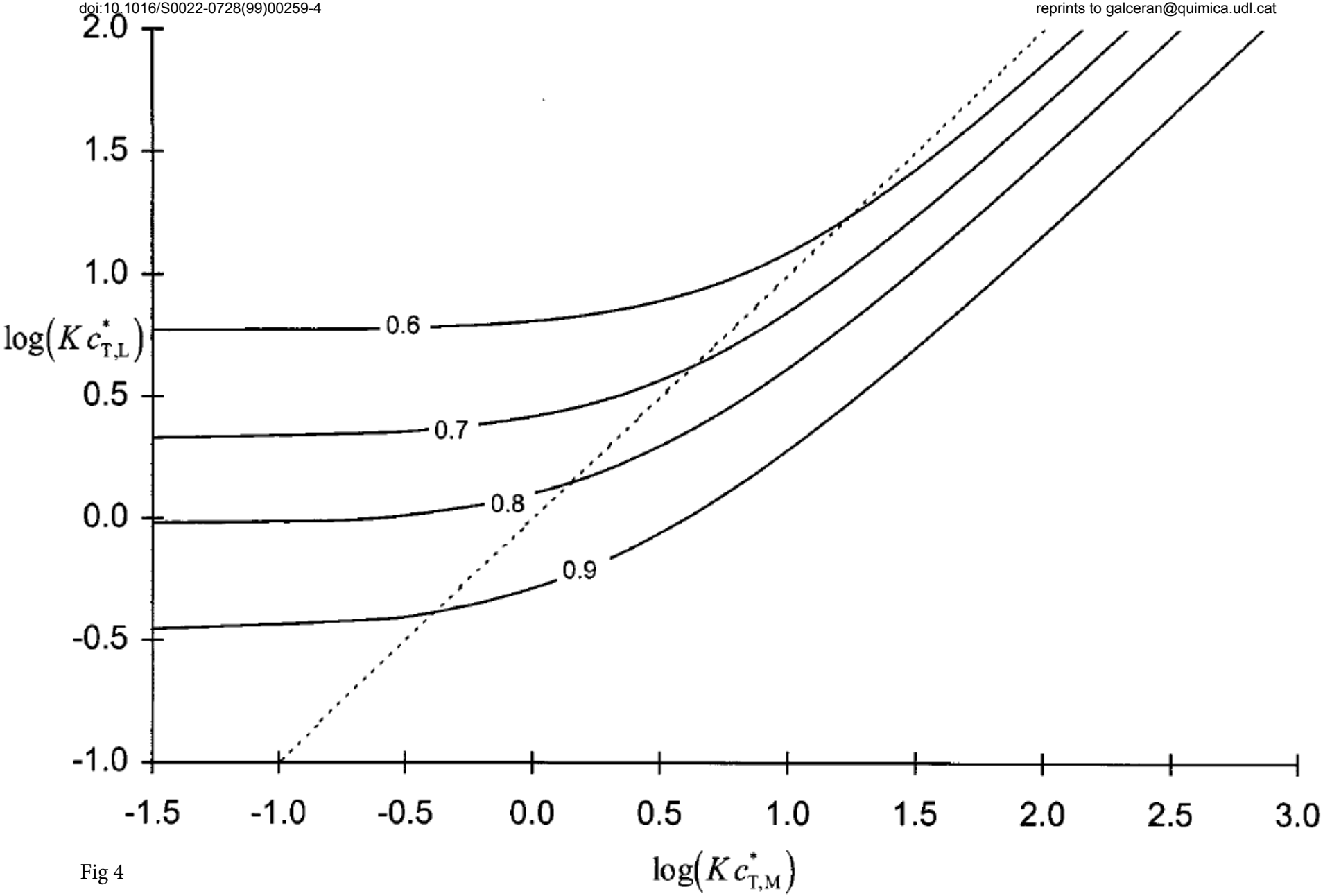

Fig 4

Published in Journal of Electroanalytical Chemistry 1999, vol 472, p 42-52
doi:10.1016/S0022-0728(99)00259-4
reprints to galceran@quimica.udl.cat

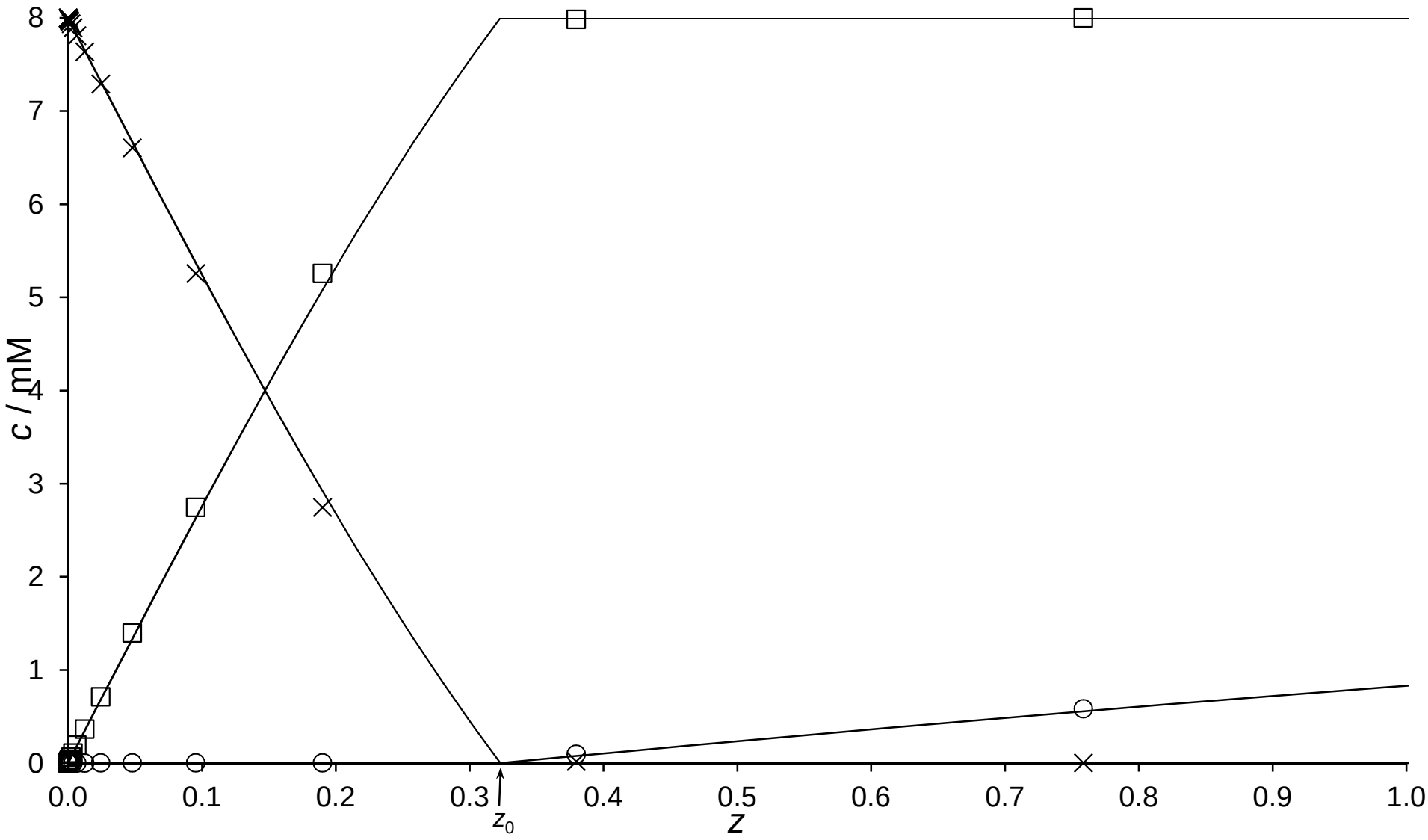

Fig 5

Published in Journal of Electroanalytical Chemistry 1999, vol 472, p 42-52
doi:10.1016/S0022-0728(99)00259-4 reprints to galceran@quimica.udl.cat

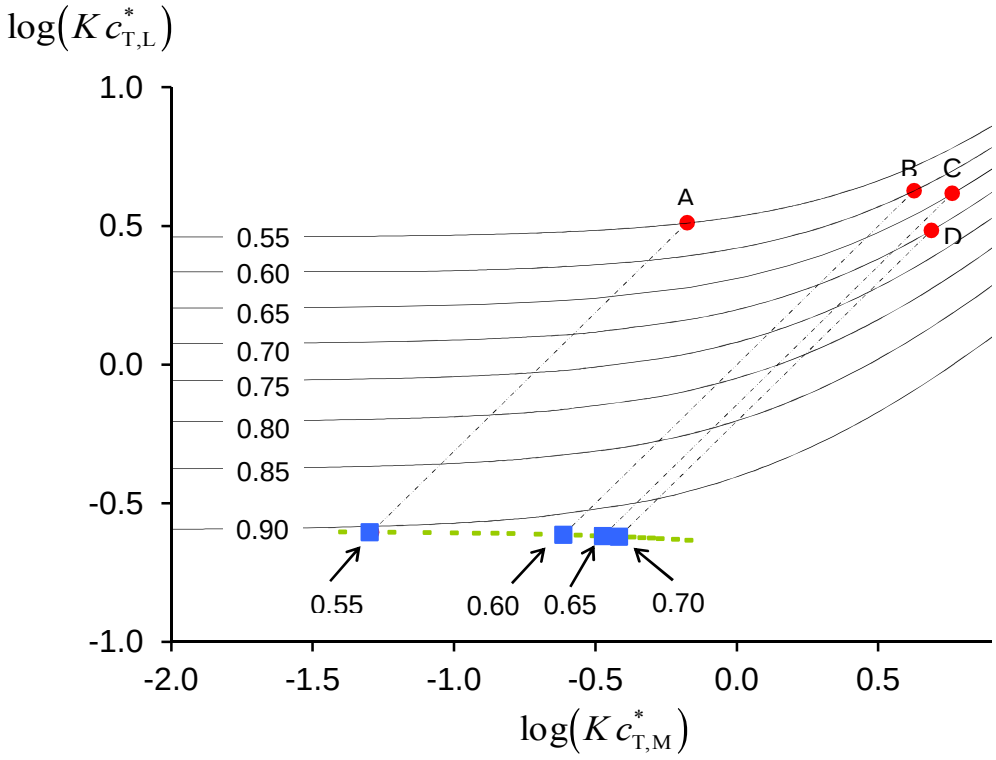

Fig 6

Published in Journal of Electroanalytical Chemistry 1999, vol 472, p 42-52
doi:10.1016/S0022-0728(99)00259-4